IEEE Access
Multidisciplinary ⋮ Rapid Review ⋮ Open Access Journal

Received 8 November 2022, accepted 24 November 2022, date of publication 28 November 2022,
date of current version 1 December 2022.

Digital Object Identifier 10.1109/ACCESS.2022.3225199

RESEARCH ARTICLE

Measurement and Analysis of Soil Temperature Field Based on Fiber Bragg Grating Sensor Array

GUOLI LI[1], HENG ZHAO[1], FEI FENG[1], QIYUE WU[1], AND BO WEI[2]
[1]School of Mechanical and Electrical Engineering, Jinling Institute of Technology, Nanjing 211169, China
[2]Wuxi Brillouin Electronic Technology Company Ltd., Wuxi 214131, China

Corresponding author: Guoli Li (qdliguoli@163.com)

This work was supported in part by the Industry–University–Research Cooperation Project of Jiangsu Province of China under Grant BY2022070, in part by the Science and Education Integration Project of Jinling Institute of Technology of China under Grant 2022KJRH05, and in part by the High-Level Talents Research Start-Up Foundation of Jinling Institute of Technology of China under Grant jit-b-202220.

ABSTRACT Studying the soil temperature field and its variation law is of great significance to the real-time service of agricultural production. To solve the problems of low detection efficiency and difficulty of distributed detection, a distributed detection method of soil temperature field using wavelength division multiplexing and space division multiplexing technologies based on fiber Bragg grating (FBG) sensor is proposed. In this scheme, the stainless steel tube encapsulating the FBG string was vertically buried in the measured soil, and the tunable laser method and the peak-seeking algorithm were used to demodulate the wavelength of each sensor of the FBG string. The soil temperature field measurement experiments were carried out in the farmland environment. The experimental results show that the proposed method can detect the soil temperature field in real time. The internal temperature of soil changes periodically with the periodic change of surface environment temperature. With the increase of depth, the influence of surface temperature on soil temperature gradually decreases, and the amplitude of soil temperature oscillation gradually decreases, but the hysteresis effect of temperature peak becomes more and more obvious. The ambient wind speed can reduce the temperature of soil surface and shallow layer. Soil moisture affects the speed of temperature transfer from the surface layer to the deep layers, and the hysteresis effect of temperature peak is more significant in the soil with higher moisture. Solar radiation has a great influence on the temperature of soil surface and shallow layer.

INDEX TERMS Fiber Bragg grating, sensor array, soil temperature field, wavelength division multiplexing, space division multiplexing.

I. INTRODUCTION

Soil temperature is an important environmental factor that directly or indirectly affects and reflects plant growth and development. On the one hand, soil temperature affects physiological processes such as plant seed germination, water and nutrient absorption, and root development [1], [2]. On the other hand, soil temperature affects chemical processes and life activities such as organic matter decomposition, nutrient transformation, and microbial activities. These activities are accompanied by the absorption and release of heat, which in turn affects the changes in soil temperature [3], [4], [5]. Soil temperature can help to forecast and understand soil ecosystem changes, and it is an important basis for determining normal crop growth. Therefore, monitoring soil temperature field and studying its variation laws are important for both real-time service and theoretical research of agricultural production.

The research of soil temperature field detection mainly includes surface temperature detection and subsurface temperature detection. Three main methods are commonly used to detect the soil temperature field:

1. The contact measurement method based on thermal resistance, thermocouples, and other electrical sensors.

The associate editor coordinating the review of this manuscript and approving it for publication was Santosh Kumar.

In this method, electric sensors are usually placed on the surface of the soil or buried in the soil at different depths for real-time temperature measurement. Han et al. [6] designed a soil sensor suitable for wireless sensor network (WSN) application system. Thermistors were used to collect soil temperature and were connected in series and parallel for non-linear error compensation or linearization. Xue et al. [7] established a soil fire temperature field model. The temperature data of each layer of soil were collected by thermocouple, and the change of soil temperature field of each layer during the fire process was obtained. The digital integrated temperature sensor DS18B20 was a single bus device, which supported multi-point networking function and could realize multi-point temperature measurement. It was widely used in the field of soil temperature detection [8], [9], [10], [11].

2. The noncontact measurement method based on visible light and infrared imaging. This method is mainly used for the measurement of soil surface temperature. Li et al. [12] studied the temperature variation laws of soil covered with different plastic films at different instants based on infrared imaging technology. Xu et al. [13] used thermal infrared remote sensing techniques to monitor soil temperature in forested area. Nicolas et al. [14] used satellite infrared remote sensing to collect snow soil temperature in permafrost areas and perform temperature retrieval.

3. The simulation measurement method based on soil temperature field prediction model. In this method, a prediction model is established to simulate the soil temperature by analyzing the relationship between the soil temperature field and meteorological factors, environmental factors [15], [16], [17], and combining the observed and recorded historical data of soil temperature. Diniz et al. [18] reformulated the mathematical model of soil temperature by inserting a variable referring to cloud cover. Wang et al. [19] proposed an embedded network prediction model based on the gated recurrent unit (GRU) model, which was used to learn the local and global features of historical temperature for improving the prediction performance of soil temperature. Doro et al. [20] developed and implemented a new cosine model and a pseudo-heat-transfer model. These new models could better predict soil temperature for a wide range of pedoclimatic conditions. Xie et al. [21] calibrated and verified the SHAW model based on the soil temperature measurement data of the last two years.

Traditional electrical sensors such as thermal resistance and thermocouples have shortcomings such as being susceptible to electromagnetic radiation, poor long-term stability and short signal transmission distance. They are not suitable for distributed measurement. The noncontact measurement method based on visible light, infrared imaging is only suitable for measuring surface or shallow soil temperature, but not for real-time measurement of subsurface soil temperature. In addition, the noncontact measuremen method requires the acquisition and processing of a large number of images. This method has complex data processing, low measurement efficiency and poor real-time performance. The third method is suitable for temperature prediction and theoretical research, and it is difficult to realize real-time temperature measurement.

Compared with traditional sensors, the fiber Bragg grating (FBG) temperature sensor has many advantages, such as small volume, antielectromagnetic interference, corrosion resistance, easy remote operation, easy multiplexing, and so on. FBGs with different center wavelengths can be engraved at different positions of the fiber to form FBG strings. By cascading multiple FBG strings, a sensor array is formed. FBG sensor array is especially suitable for distributed multipoint measurement and structural health monitoring [22], [23]. In recent years, researchers have carried out a lot of research on the application of temperature and soil moimsture measurement with FBG sensor array [24], [25], [26], [27], [28], [29], [30].

To solve the above problems, a distributed detection method of soil temperature field based on FBG sensor array was proposed. FBG sensor array based on wavelength division multiplexing and space division multiplexing technologies is arranged at different depths of soil for multi-layer real-time temperature measurement. The distribution law, variation law of soil temperature field and its relationship with solar radiation power, soil moisture, wind speed and other factors were studied. This method improves the measurement efficiency of soil temperature, and also provides a reference for the measurement of space temperature field in other fields.

II. SOIL TEMPERATURE FIELD ANALYSIS

Soil temperature and its distribution depend on the heat exchange process of the soil. The sources of soil heat include solar radiation heat, heat generated in the earth's interior, and heat released by biological and chemical processes in the soil. Among them, solar radiation heat is the main source of soil heat. The soil heat is exported to the outside world in various ways, including radiation on the soil surface, convection, evaporation, plant transpiration, and conduction to the depths of the ground. The external factors affecting heat exchange include air density, temperature and moisture, ambient wind speed, terrain, ground cover, etc. The internal factors include soil composition, structure, moisture, color, etc.

Since solar radiation is the main source of soil heat, the soil temperature has daily and annual cycle variations due to the cyclical changes in solar radiation. This paper studies the daily variation of soil temperature.

The main form of heat transfer in soil is thermal conduction. It is assumed that the soil is a homogeneous isotropic medium. Its thermal properties do not change with depth, and there is no heat exchange along the horizontal direction. Therefore, the calculation of soil natural temperature field can be simplified as one-dimensional periodic heat conduction problem of semi-infinite body under the third boundary condition [31], [32]. The unsteady heat conduction equation

of soil natural temperature field is:

$$\frac{\partial t(x,\tau)}{\partial \tau} = a\frac{\partial^2 t(x,\tau)}{\partial x^2} \tag{1}$$

where τ is the time, x is the depth below the soil surface, $t(x,\tau)$ is the soil temperature at time τ and at depth x, a is the soil thermal diffusivity. a is a physical quantity that expresses the speed of soil temperature change under the condition of certain heat gain and loss, which can be calculated by the following formula:

$$a = \frac{\gamma}{C_g} = \frac{\gamma}{\rho C_p} \tag{2}$$

where C_g is soil volumetric heat capacity, γ is soil thermal conductivity, ρ is soil density, C_p is soil specific heat. The relationship between soil thermal diffusivity and soil moisture is complex, because the soil moisture affects both soil thermal conductivity and volumetric heat capacity. According to experiments and observations, in the case of low soil moisture, the soil thermal diffusivity increases with the increase of soil moisture. However, when the soil moisture exceeds a certain value, the thermal conductivity of the soil does not increase significantly, and the heat capacity still increases linearly with the moisture, so the soil thermal diffusivity decreases instead. If the initial state temperature distribution of the soil is not considered, the boundary conditions of the above soil heat conduction equation are:

$$\left.\begin{aligned} t(x,\tau)\,|_{x=0} &= t(0,\tau) \\ t(x,\tau)\,|_{x=\delta} &= T_a \end{aligned}\right\} \tag{3}$$

where δ is the depth of the soil constant temperature layer, T_a is the temperature of the soil constant temperature layer, which is approximately equal to the average soil surface temperature.

If the ambient temperature does not change suddenly, the temperature of the soil surface will not jump greatly. It is assumed that the diurnal variation of soil surface temperature is in the form of a simple harmonic function:

$$t(0,\tau) = T_a + T_m \cos(\frac{2\pi}{\tau_0}\tau) \tag{4}$$

where τ_0 is the fluctuation period, which is 24 hours for the daily variation, T_m is the amplitude of soil surface temperature fluctuations above and below the average T_a.

According to Equations (1), (3) and (4), the theoretical calculation model of soil temperature field at different depths and at different times can be obtained by using the separation variable method:

$$t(x,\tau) = T_a + T_m \exp(-x\sqrt{\frac{\pi}{a\tau_0}})\cos(\frac{2\pi}{\tau_0}\tau - x\sqrt{\frac{\pi}{a\tau_0}}) \tag{5}$$

It can be seen from Equation (5) that the variation of soil temperature at the depth x is similar to the variation of surface temperature, and they are both cosine functions with the same period. However, the amplitude of soil temperature fluctuation below the surface decays rapidly and exponentially with depth. When reaching a certain depth, the fluctuation amplitude of soil temperature is very small. Below this depth, the soil temperature can be seen to remain constant, known as the isothermal layer. The time when the soil temperature at x depth reaches the peak value lags behind the time when the soil surface temperature reaches the peak value. The lag time can be calculated by equation $x\sqrt{\tau_0/\pi a}/2$.

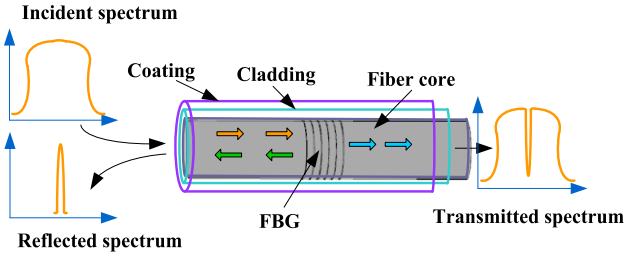

FIGURE 1. Functional principle of FBG.

III. SOIL TEMPERATURE MEASUREMENT MECHANISM BASED ON FBG SENSOR ARRAY

A. FBG TEMPERATURE SENSING PRINCIPLE

FBG is a diffraction grating formed by periodically modulating the refractive index of the fiber core in the axial direction. It can reflect light of specific wavelength, which is the FBG Bragg wavelength λ_B, shown in Fig. 1.

The Bragg wavelength λ_B is related to the grating period Λ and the effective refractive index n_{eff} of the fiber core, shown in Equation (6):

$$\lambda_B = 2n_{eff}\Lambda \tag{6}$$

If the FBG temperature changes, the photothermal effect caused by the temperature change causes the effective refractive index to change and the thermal expansion coefficient causes the grating constant to change. The relative displacement of the Bragg wavelength caused by temperature change is:

$$\begin{aligned} \frac{\Delta\lambda_B}{\lambda_B} &= \frac{1}{\Lambda}\frac{\partial\Lambda}{\partial T}\Delta T + \frac{1}{n_{eff}}\frac{\partial n_{eff}}{\partial T}\Delta T \\ &= (\alpha+\xi)\Delta T = K_T\Delta T \end{aligned} \tag{7}$$

where $\alpha = \frac{1}{\Lambda}\frac{\partial\Lambda}{\partial T}$ is the thermal expansion coefficient of optical fiber, $\xi = \frac{1}{n_{eff}}\frac{\partial n_{eff}}{\partial T}$ is the thermal optical coefficient of optical fiber, K_T is the temperature sensitivity coefficient of the relative wavelength.

If FBG is subjected to axial strain ε_z, the photoelastic effect causes the refractive index to change, which causes the Bragg wavelength shift:

$$\frac{\Delta\lambda_B}{\lambda_B} = (1-P_e)\varepsilon_z = K_\varepsilon\varepsilon_z \tag{8}$$

where $P_e = n_{eff}^2[P_{12} - \upsilon(P_{11}+P_{12})]/2$, P_{11} and P_{12} are the elastic optic coefficient, υ is optical fiber Poisson's ratio, K_ε is the relative wavelength strain sensitivity coefficient of the FBG.

According to Equations (7) and (8), the relationship between the change in the grating Bragg wavelength and the

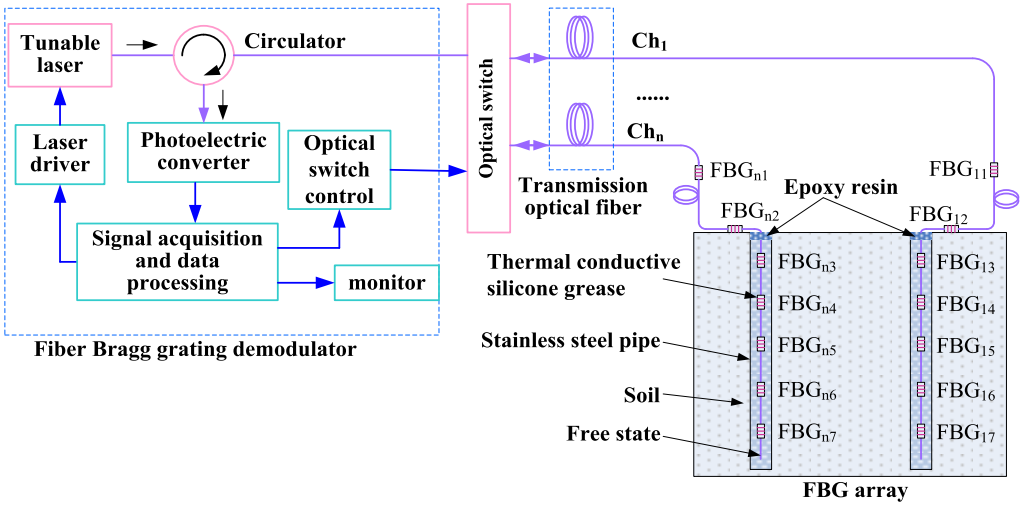

FIGURE 2. Structure of soil temperature measurement system based on FBG array.

change in temperature and axial strain is:

$$\frac{\Delta\lambda_B}{\lambda_B} = (\alpha + \xi)\Delta T + (1 - P_e)\varepsilon_z \tag{9}$$

Therefore, if measures are taken to prevent FBG from being disturbed by stress, there is a linear relationship between $\Delta\lambda_B$ and ΔT. The temperature change can be determined by detecting the displacement of the Bragg wavelength.

B. SOIL TEMPERATURE MEASUREMENT SYSTEM BASED ON FBG ARRAY

The structure of the distributed soil temperature measurement system based on FBG array was shown in Fig. 2. It was constructed by the wavelength division multiplexing and space division multiplexing technology.

Seven FBGs with different Bragg wavelengths were connected in series on one transmission fiber. FBG_{n1} and FBG_{n2} were used to measure the ambient air temperature and soil surface temperature respectively, and FBG_{n3}-FBG_{n7} were used to measure the temperature of multi-layer soil under the surface.

The FBG_{n3}-FBG_{n7} sensor string was coated with uncured diluted thermal conductive silicone grease and then placed into a stainless steel tube. This ensured the mechanical strength of the FBG sensor string. The thermal conductive silicone grease was used to fully fill the gap between the optical fiber and the stainless steel pipe wall to ensure the uniformity of FBGs temperature. This could also avoid the influence of soil moisture, water vapor and other factors on FBG temperature measurement. The thermal conductive silicone grease used can maintain the paste state at −50 °C-230 °C without solidifying or adhesive force, and it can avoid uneven heating of the FBG.

The upper end of the stainless pipe was filled with epoxy resin to seal the stainless steel gate and fix the optical fiber. The tail of FBG sensor string was kept free to avoid the interference of stress on FBGs during temperature measurement. FBG_{n1} and FBG_{n2} were also in a relaxed state.

The wavelength of the narrow-band light source output by the tunable laser could vary within a certain range. The laser scanning step size and frequency could be controlled by the driver. A narrow-band laser was emitted to an FBG array through a circulator. Different sensing channels could be selected through the optical switch. When the light source wavelength was consistent with the Bragg wavelength of an FBG, the reflected signal light intensity was maximum. The reflected light signal reached the photoelectric converter through the circulator, and it was converted into an electrical signal. The data processing computer collected the electrical signal, and the signal voltage peak was obtained by the peak-seeking algorithm. The measured temperature and FBG positioning could be determined by comparing the Bragg wavelength of each FBG and its variation.

IV. FBG CALIBRATION AND EXPERIMENTAL EQUIPMENT

A. FBG CALIBRATION

Two FBG sensor strings were used in the experiment, and each string was engraved with 7 FBGs, a total of 14 FBGs. The length of the FBG grating area was 10 mm, the 3 dB bandwidth was 0.209 nm-0.232 nm, the reflectivity was greater than 92%, and the length of the transmission fiber was 15 m. In the experiment, the Bragg wavelengths of FBG_{11}-FBG_{17} are 1532.039 nm, 1536.135 nm, 1538.948 nm, 1542.733 nm, 1545.953 nm, 1548.217 nm, 1552.268 nm respectively at 25 °C, the Bragg wavelengths of FBG_{21}- FBG_{27} are 1532.266 nm, 1536.134 nm, 1539.817 nm, 1543.784 nm, 1547.325 nm, 1553.266 nm, 1557.993 nm respectively at 25 °C.

Before the experiment, it was necessary to recalibrate the temperature sensitivity coefficient of each FBG. The FBG sensor string to be calibrated was put into a temperature control chamber. The temperature of the control chamber was set from 10 °C-70 °C. The Bragg wavelengths of the FBGs

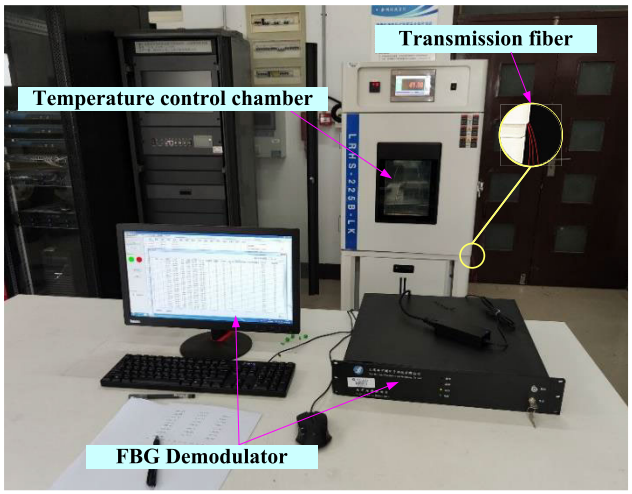

FIGURE 3. FBG calibration experiment.

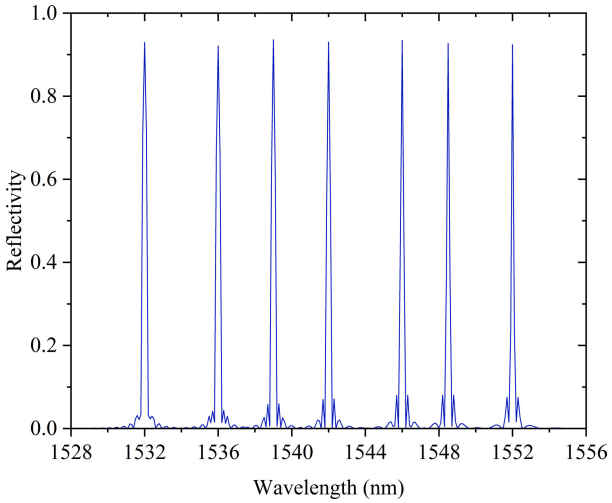

FIGURE 4. Reflection spectrum of FBG_{11}-FBG_{17} at 20 °C.

were recorded every 10 °C, as shown in Fig. 3. Based on the measured Bragg wavelength and parameters of each FBG, the reflection spectrum of the FBG string could be plotted. Fig. 4 showed the reflection spectrum of FBG_{11}-FBG_{17} at 20 °C. The calibration curves were shown in Fig. 5. The calibration results showed that the temperature change of each FBG was basically linear with the Bragg wavelength displacement in the measured temperature range. The temperature sensitivity coefficient of each FBG sensor is greater than 10 pm/°C.

B. EXPERIMENTAL MATERIALS AND EQUIPMENT

The experimental system was mainly composed of two FBG sensor strings, a FBG demodulator, two soil moisture meters, a solar power meter and an anemometer. The equipment models were shown in Table 1. The FBG demodulator was shown in Figure 3, and its wavelength band was 1525 nm-1565 nm, the scanning frequency was 100 Hz, and the wavelength resolution was 1 pm. Based on this demodulator, the FBG array was used to measure the surface temperature of photovoltaic module by the author, the measurement results were basically consistent with those of contact electrical sensor and infrared thermal imager [27]. The soil moisture meter was used to measure the moisture of each layer of soil, as shown in Fig. 6. In addition, the anemometer and solar power meter were used to measure wind speed and solar power, respectively.

Before the experiment, the stainless steel tubes packaged with FBG string were vertically embedded in the measured soil. FBG_{n3}-FBG_{n7} were used to measure soil temperature at 5 cm, 15 cm, 25 cm, 35 cm, and 45 cm below the surface, respectively. The moisture sensor probes were arranged near each FBG buried underground to measure the soil moisture at the corresponding position. The anemometer and solar power meter were placed on the surface of the measuring point.

V. EXPERIMENT AND RESULT ANALYSIS

The geographic location of the experiment was latitude 31°44'3'' N, longitude 118°49'51'' E, and altitude 6 m. The measuring object was farmland soil, and the soil type was red soil.

A. MEASUREMENT AND ANALYSIS OF DAILY VARIATION OF SOIL TEMPERATURE FIELD

The packaged FBG sensor string was buried in the soil 72 hours before the measurement. The measurement area was well watered so that the soil was in full contact with the sensor probe. The measurements were taken from July 24 at 8:50 to July 25 at 9:50, with data collected at 2-minute intervals. During the measurement, the weather was mainly sunny, occasionally cloudy, the maximum wind speed was 1.05 m/s, the average wind speed was 0.082 m/s. The wind speed had little effect on the soil temperature.

The measurement results were shown in Fig. 7. T05, T15, T25, T35, T45 were the soil temperatures at depths of 5 cm, 15 cm, 25 cm, 35 cm, and 45 cm, respectively. T00 was the surface temperature of the measurement point, and Ta was the air temperature.

The measurement results were analyzed as follows:

(1) The daily curves of atmospheric temperature and shallow soil temperature were close to the cosine function model with a period of 24 h. The temperature of the deep soil layer (below 45 cm) is basically at a constant temperature.

(2) With the increase of depth, the influence of surface temperature on soil temperature decreased gradually, and the oscillation amplitude decreased gradually, but the hysteresis effect of temperature peak was more and more obvious.

(3) The daily variation of soil temperature showed the characteristics of alternating changes in the values of the upper and lower soil layers. During the daytime, the soil temperature gradually decreased from the surface layer to the deep layer, and the opposite was true at night.

The above experimental results are basically consistent with the results of the aforementioned theoretical analysis of soil temperature field. However, affected by solar radiation and air flow changes, the frequency and amplitude

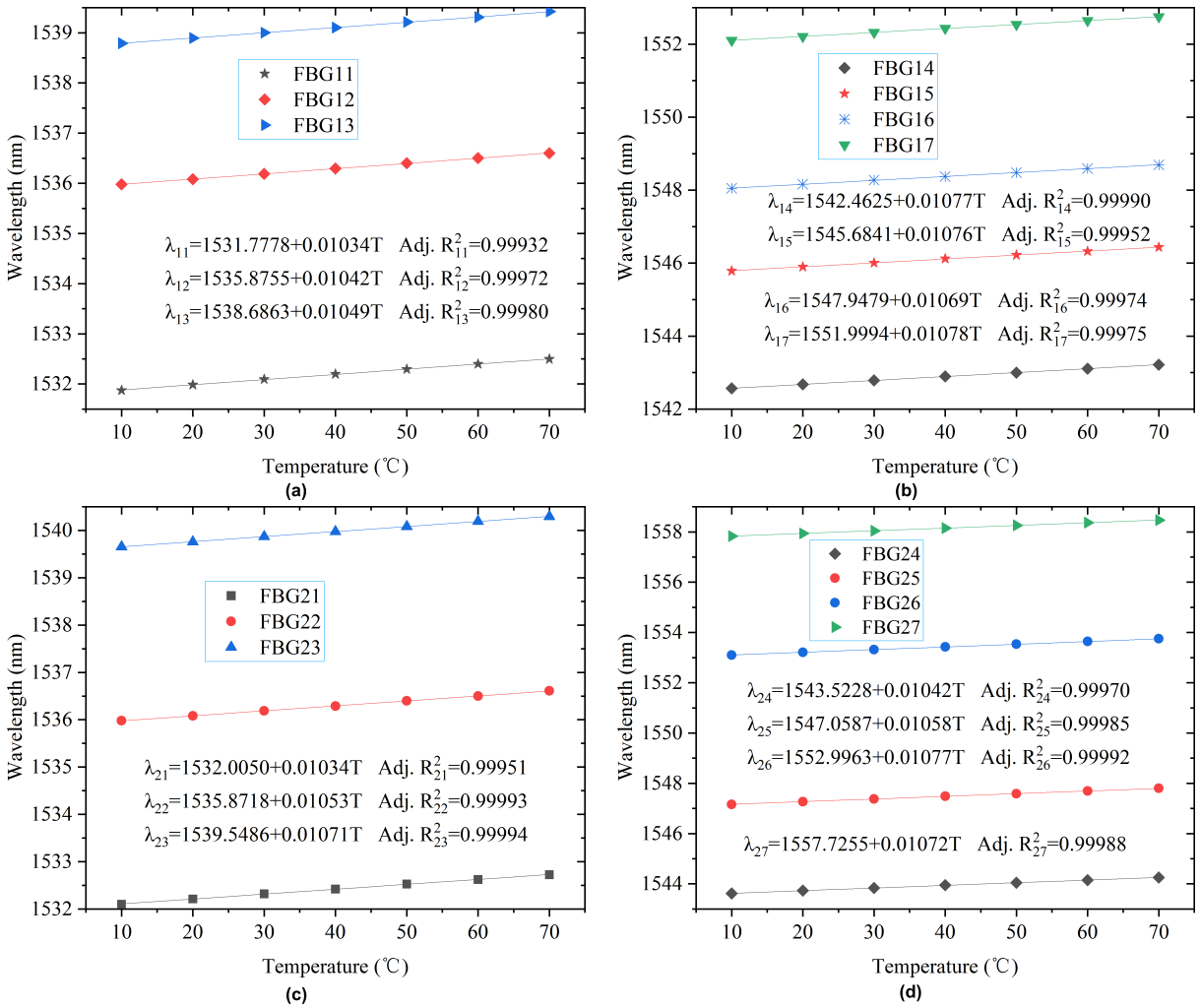

FIGURE 5. Calibration curves of FBGs. (a) FBG_{11}-FBG_{13}. (b) FBG_{14}-FBG_{17}. (c) FBG_{21}-FBG_{23}. (d) FBG_{24}-FBG_{27}.

TABLE 1. Experimental equipment.

Equipment	Model	Manufacturer
FBG demodulator	BLY-FBG-5S	China Wuxi Brillouin Electronic Technology Co., Ltd.
Soil moisture meter	RS-N01-TR-5	China Shandong Renke measurement and Control Technology Co., Ltd.
Solar power meter	TES-1333R	China TES Electrical Electronic Corp
Anemometer	Benetech GM8907	China Shenzhen Jumaoyuan Science And Technology Co., Ltd.

of atmospheric and surface temperature fluctuations in the daytime were higher, and the ripple of temperature curves at night were less.

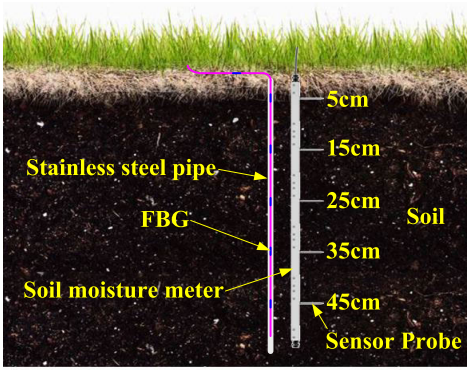

FIGURE 6. Schematic diagram of the arrangement of FBG and moisture meter in the soil.

B. INFLUENCE OF SOIL MOISTURE ON TEMPERATURE FIELD

The two packaged FBG sensor strings were buried in two areas to be measured, A and B. The two experimental areas were watered to different degrees so that the soil moisture was significantly different in the two areas. The measurement period was from 9:00 on August 19 to 9:00 on August 20, and the data were collected every 2 minutes. During the measurement, the weather was mainly sunny, the gust was level 2. The wind speed had little effect on the soil temperature. The measurement results were shown in Fig. 8 and Fig. 9.

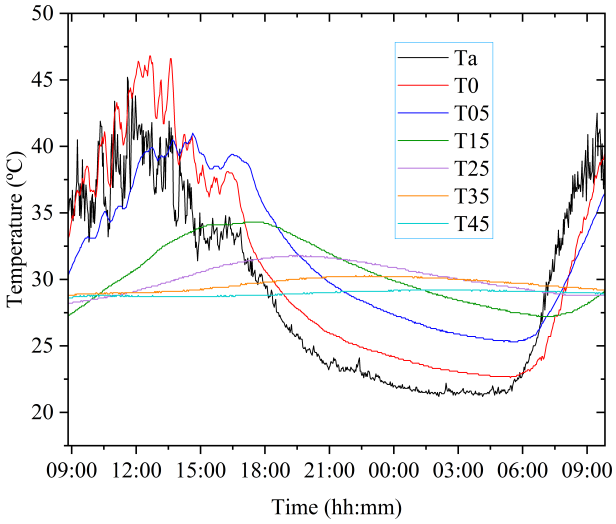

FIGURE 7. Measurement results of daily variation of soil temperature field.

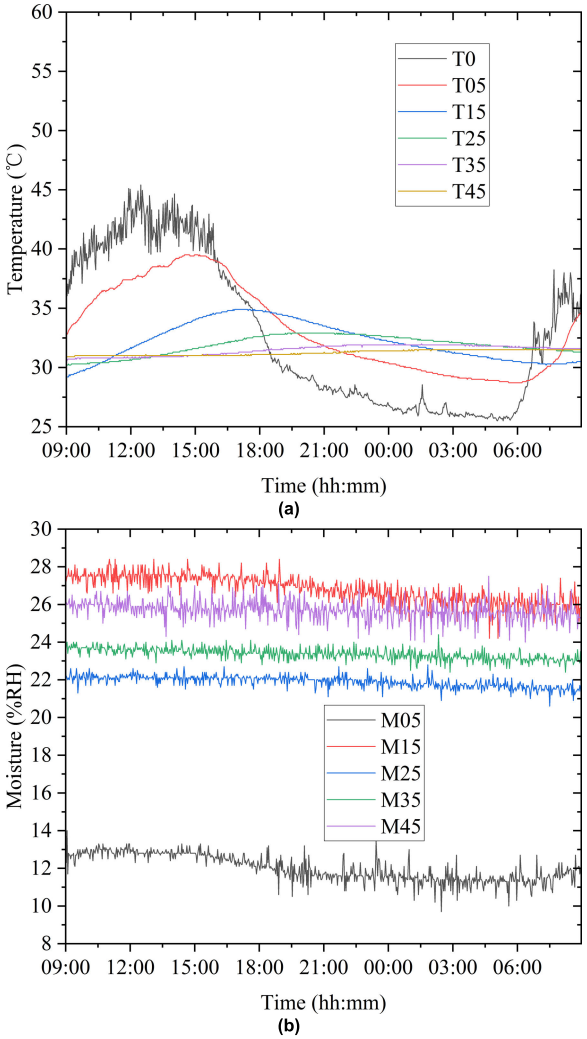

FIGURE 8. Measurement results of soil temperature field and soil moisture in area A. (a) soil temperature. (b) soil moisture.

M05, M15, M25, M35, M45 were soil moistures at depths of 5 cm, 15 cm, 25 cm, 35 cm, and 45 cm, respectively.

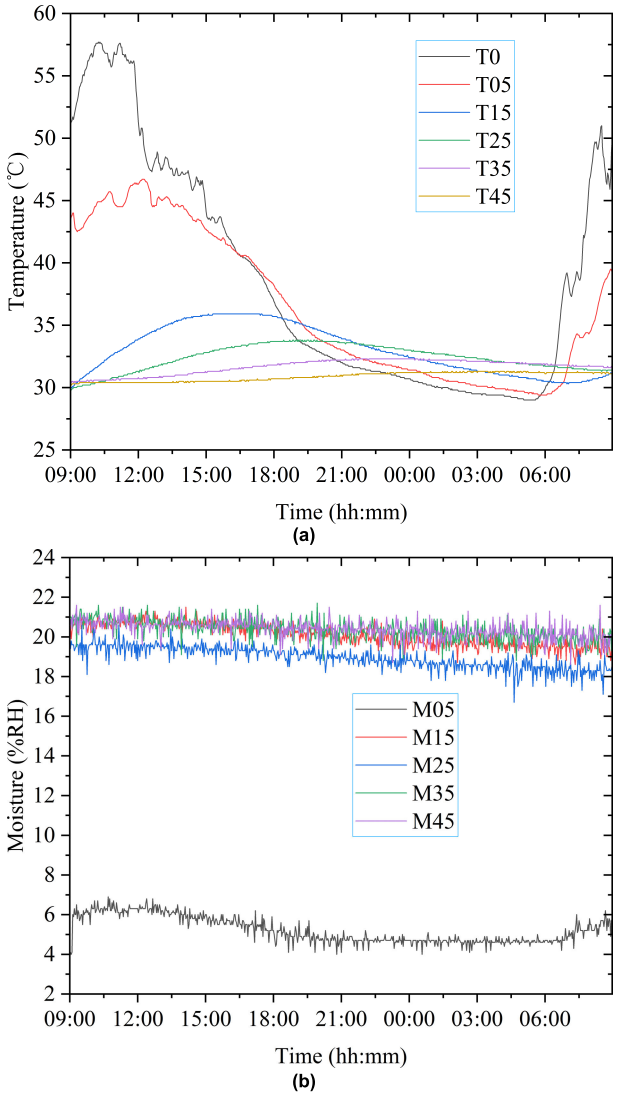

FIGURE 9. Measurement results of soil temperature field and soil moisture in area B. (a) soil temperature. (b) soil moisture.

By analyzing the measurement results in Figures 8 and 9, it could be seen that:

(1) The higher the soil moisture, the more surface water evaporated, which was conducive to the heat dissipation of the surface and shallow soil. Within a certain moisture range, the higher the soil moisture, the lower the surface and shallow soil temperatures. Soil moisture had less effect on deep soil temperatures.

(2) Soil moisture affected the speed of heat transfer from the surface layer to the deep layer. In summer, compared with the soil with medium moisture, the hysteresis effect of temperature peak in the soil with high moisture was more significant.

C. INFLUENCE OF SOLAR RADIATION POWER ON TEMPERATURE FIELD

Before the experiment, two places A and B were irrigated to the same degree so that their soil moisture levels were

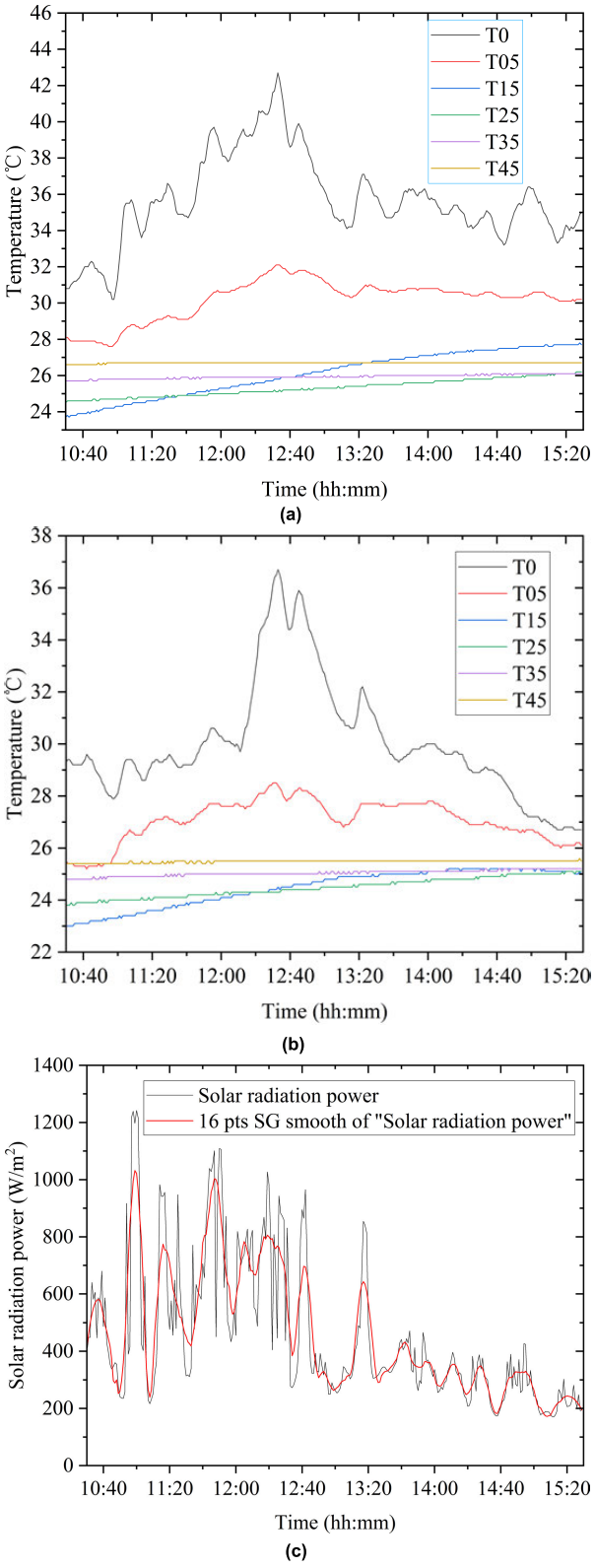

FIGURE 10. Influence of solar radiation power on soil temperature field. (a) measurement results of area A. (b) measurement results of area B. (c) measurement results of solar radiation power.

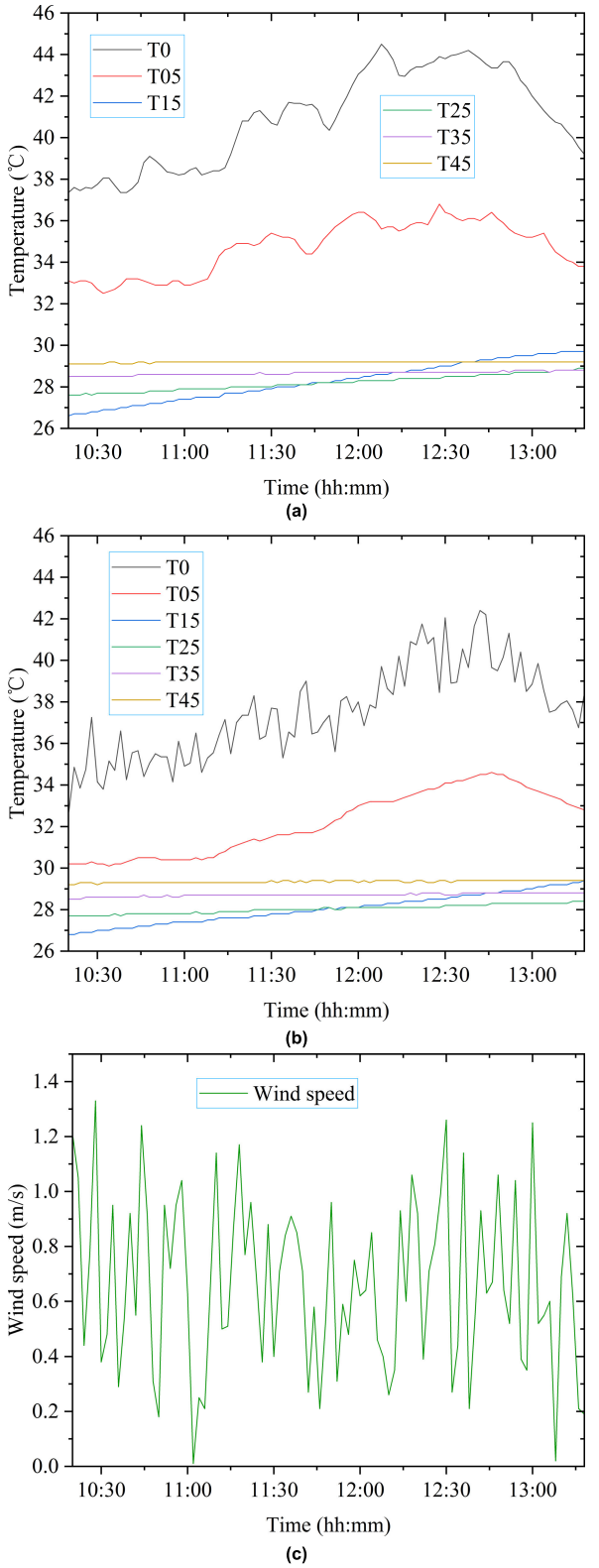

FIGURE 11. Influence of wind speed on soil temperature field. (a) measurement results of area A. (b) measurement results of area B. (c) measurement results of simulate wind speed.

essentially the same. 72 hours before the measurement, the B area was shielded from the sun by a sunshade net. The measurement experiment was carried out from 10:30 a.m. to 15:30 p.m. with an interval of 1 minutes to collect data.

During the measurement, the weather was sunny and cloudy. The measurement results were shown in Fig. 10.

By analyzing the measurement results in Fig. 10, it could be seen that:

(1) The solar radiation power fluctuated frequently due to the cloud cover. Affected by the fluctuation of solar radiation power, the soil surface temperature fluctuated significantly, and the fluctuation frequency of both fluctuations was basically the same.

(2) The shading of solar radiation by the sunshade net reduced the soil temperature, and had a great impact on the temperature of the soil surface and shallow layer.

D. INFLUENCE OF AMBIENT WIND SPEED ON TEMPERATURE FIELD

Before the experiment, two places A and B were irrigated to the same degree to make the soil moisture basically the same. A fan was used to circulate air in the B area to simulate natural wind. The fan started to run at 10:00 on August 26, and the soil temperature was measured from 10:20 on August 26 to 13:20 on August 26. During the experiment period, the weather was cloudy with gust of level 1. Natural wind had little effect on soil temperature. The measurement results were shown in Fig. 11.

Wind speed could accelerate convective heat exchange between soil and atmosphere, promote evaporation of water from the soil surface, accelerate heat dissipation, and lower soil temperature. The analysis of the measurement results in Fig. 11 showed that the wind speed had a greater effect on the surface and shallow soil temperature, but had little effect on the deeper soil.

VI. CONCLUSION

A soil temperature field detection system based on distributed FBG sensor array was designed by combining wavelength division multiplexing technology and space division multiplexing technology. The stainless steel tubes packaging the fiber grating string were vertically buried in the soil to be measured, and the tunable laser method and the peak-seeking algorithm were used to demodulate the wavelength displacement of each sensor in the FBG string. An experimental platform was built to carry out soil temperature measurement experiments in the farmland environment. The experimental results are as follows:

1. The temperature sensitivity coefficient of the FBG sensor of this detection method is greater than 10 pm/° C, and the response time of the sensing probe is short. The detection system can obtain the multi-layer temperature distribution of soil in real time.

2. The temperature inside the soil changes periodically with the periodic change of surface environment temperature. With the increase of depth, the influence of surface temperature on soil temperature gradually decreases, the oscillation amplitude decays approximately exponentially and eventually tends to be constant, but the hysteresis effect of temperature peaks is becoming more and more obvious.

3. The daily variation of soil temperature shows the characteristics of alternating changes in the values of the upper and lower soil layers. The rate of change of surface soil temperature is much greater than that of deep soil temperature. In summer, the temperature of the surface and the shallow layer is significantly higher than that of the deep layer in the daytime, but the opposite is true at night.

4. Soil moisture affectes the speed of heat transfer from the surface layer to the deep layer. Within a certain moisture range, the higher the soil moisture, the lower the surface and shallow soil temperatures. Soil moisture has less effect on deep soil temperature values. The fluctuation of solar radiation has a great influence on the temperature of surface and shallow layer soil. Wind speed can reduce the temperature of surface and shallow soil, but has little effect on the temperature of deep soil.

Soil temperature is closely related to crop growth. In this paper, the FBG sensor array was used to realize the real-time detection of soil temperature, and the relationship between temperature field changes and environmental parameters was obtained. This laid a foundation for taking effective measures to control soil temperature and keeping it at a moderate value. The influence of environmental parameters on the soil temperature field is coupled and complex. How to obtain environmental parameter information from soil temperature field information through data analysis and data mining is one of the future research directions.

REFERENCES

[1] M. N. Rahman, R. Hangs, and J. Schoenau, "Influence of soil temperature and moisture on micronutrient supply, plant uptake, and biomass yield of wheat, pea, and Canola," *J. Plant Nutrition*, vol. 43, no. 6, pp. 823–833, Apr. 2020.

[2] X. Zhang, R. Guo, W. Li, X. Qiao, and W. Zheng, "Design and experiment of assembled soil temperature sensor," *Trans. Chin. Soc. Agricult. Eng.*, vol. 31, no. 1, pp. 205–211, Jan. 2015.

[3] Y. Yi, Y. Liang, and D. Zhang, "Effect of irrigation and fertilization on temperature and CO_2 content of greenhouse soil," *Chin. J. Soil Sci.*, vol. 37, no. 5, pp. 875–880, Oct. 2006.

[4] M. Yan, Z. Li, X. Tian, L. Zhang, and Y. Zhou, "Improved simulation of carbon and water fluxes by assimilating multi-layer soil temperature and moisture into process-based biogeochemical model," *Forest Ecosyst.*, vol. 6, no. 1, pp. 1–15, Dec. 2019.

[5] P. Baldrian, J. Šnajdr, V. Merhautová, P. Dobiášová, T. Cajthaml, and V. Valášková, "Responses of the extracellular enzyme activities in hardwood forest to soil temperature and seasonality and the potential effects of climate change," *Soil Biol. Biochem.*, vol. 56, pp. 60–68, Jan. 2013.

[6] Y. Han, B. Zhao, and N. Wu, "Design of soil salt-moisture-temperature sensor for WSN," *Instrum. Technique Sensor*, no. 11, pp. 5–9, Jan. 2016.

[7] W. Xue, C. Sha, H. Zhang, and D. Guo, "Experimental study on soil fire temperature field of harvested site of Larix olgensis plantation," *Chin. J. Appl. Ecol.*, vol. 30, no. 3, pp. 785–792, Mar. 2019.

[8] X. Zhang, C. Zhang, J. Fang, X. Yu, and J. Liang, "Smart sensor nodes for wireless soil temperature monitoring system in precision agriculture," *Trans. Chin. Soc. Agricult. Machinery*, vol. 40, no. 9, pp. 237–240, Sep. 2009.

[9] J. Li, Z. Du, and H. Tian, "Experimental study on soil temperature field of earth-air heat exchanger in solar greenhouse," *Acta Energiae Solaris Sinica*, vol. 42, no. 12, pp. 375–380, Dec. 2021.

[10] S. Susilawati and I. Maulana, "Soil quality monitoring prototype with humidity and temperature parameters for paddy plants," *Jurnal Neutrino*, vol. 12, no. 1, pp. 14–20, Jan. 2020.

[11] Z. Xie, P. Wu, G. Han, C. Xuan, and D. Han, "Soil temperature detection system based on ZigBee technology research," *J. Agricult. Mechanization Res.*, vol. 35, no. 2, pp. 189–191, Feb. 2013.

[12] X. Li, Y. Guo, Z. Ding, X. Leng, T. Tian, and Q. Hu, "Influence of different film mulchings on soil temperature at different time scales and maize yield," *Trans. Chin. Soc. Agricult. Machinery*, vol. 49, no. 9, pp. 247–256, Sep. 2018.
[13] C. Xu, J. J. Qu, X. Hao, Z. Zhu, and L. Gutenberg, "Surface soil temperature seasonal variation estimation in a forested area using combined satellite observations and in-situ measurements," *Int. J. Appl. Earth Observ. Geoinf.*, vol. 91, Sep. 2020, Art. no. 102156.
[14] N. Marchand, A. Royer, G. Krinner, A. Roy, A. Langlois, and C. Vargel, "Snow-covered soil temperature retrieval in Canadian Arctic permafrost areas, using a land surface scheme informed with satellite remote sensing data," *Remote Sens.*, vol. 10, no. 11, p. 1703, Oct. 2018.
[15] X. Tan, S. Luo, H. Li, X. Hao, J. Wang, Q. Dong, and Z. Chen, "Investigating the effects of snow cover and vegetation on soil temperature using remote sensing indicators in the three river source region, China," *Remote Sens.*, vol. 14, no. 16, p. 4114, Aug. 2022.
[16] L. Penghui, A. A. Ewees, B. H. Beyaztas, C. Qi, S. Q. Salih, N. Al-Ansari, S. K. Bhagat, Z. M. Yaseen, and V. P. Singh, "Metaheuristic optimization algorithms hybridized with artificial intelligence model for soil temperature prediction: Novel model," *IEEE Access*, vol. 8, pp. 51884–51904, 2020.
[17] Q. Li, Y. Zhao, and F. Yu, "A novel multichannel long short-term memory method with time series for soil temperature modeling," *IEEE Access*, vol. 8, pp. 182026–182043, 2020.
[18] J. M. T. Diniz, C. A. C. D. Santos, J. P. S. D. Silva, and Á. B. D. Rocha, "Reformulation of the used model to estimate soil temperature," *Energies*, vol. 15, no. 8, p. 2905, Apr. 2022.
[19] X. Wang, W. Li, and Q. Li, "A new embedded estimation model for soil temperature prediction," *Sci. Program.*, vol. 2021, pp. 1–16, Jul. 2021.
[20] L. Doro, X. Wang, C. Ammann, M. D. A. Migliorati, T. Grünwald, K. Klumpp, B. Loubet, E. Pattey, G. Wohlfahrt, J. R. Williams, and M. L. Norfleet, "Improving the simulation of soil temperature within the EPIC model," *Environ. Model. Softw.*, vol. 144, Oct. 2021, Art. no. 105140.
[21] T. Xie, Y. Ma, and C. Yang, "Simulation of soil temperature in Qinghai lake watershed by SHAW model," *Soils*, vol. 54, no. 1, pp. 161–168, Feb. 2022.
[22] M. M. Elgaud, A. A. A. Bakar, A. A. Ghaith, N. F. Naim, N. Arsad, M. H. H. Mokhtar, N. H. Azeman, and M. S. D. Zan, "Pulse compressed time domain multiplexed fiber Bragg grating sensor: A comparative study," *IEEE Access*, vol. 6, pp. 64427–64434, 2018.
[23] R. Min, Z. Liu, L. Pereira, C. Yang, Q. Sui, and C. Marques, "Optical fiber sensing for marine environment and marine structural health monitoring: A review," *Opt. Laser Technol.*, vol. 140, Aug. 2021, Art. no. 107082.
[24] G. Li, F. Feng, F. Wang, and B. Wei, "Temperature field measurement of photovoltaic module based on fiber Bragg grating sensor array," *Materials*, vol. 15, no. 15, p. 5324, Aug. 2022.
[25] Y. Hao, Y. Fu, J. Wei, L. Yang, G. Mao, Z. Yang, and L. Li, "Internal temperature detections of contaminated silicone rubber under discharge conditions based on fiber Bragg gratings," *IEEE Access*, vol. 7, pp. 161167–161174, 2019.
[26] F. Jasmi, N. H. Azeman, A. A. A. Bakar, M. S. D. Zan, K. H. Badri, and M. S. Su'ait, "Ionic conductive polyurethane-graphene nanocomposite for performance enhancement of optical fiber Bragg grating temperature sensor," *IEEE Access*, vol. 6, pp. 47355–47363, 2018.
[27] G. Li, F. Wang, F. Feng, and B. Wei, "Hot spot detection of photovoltaic module based on distributed fiber Bragg grating sensor," *Sensors*, vol. 22, no. 13, p. 4951, Jun. 2022.
[28] J. Kumar, O. Prakash, S. K. Agrawal, R. Mahakud, A. Mokhariwale, S. K. Dixit, and S. V. Nakhe, "Distributed fiber Bragg grating sensor for multipoint temperature monitoring up to 500°C in high-electromagnetic interference environment," *Opt. Eng.*, vol. 55, no. 9, Sep. 2016, Art. no. 090502.
[29] H. Wang, S. Gao, X. Yue, X. Cheng, Q. Liu, R. Min, H. Qu, and X. Hu, "Humidity-sensitive PMMA fiber Bragg grating sensor probe for soil temperature and moisture measurement based on its intrinsic water affinity," *Sensors*, vol. 21, no. 21, p. 6946, Oct. 2021.
[30] C. Li, J. Tang, Y. Jiang, C. Cheng, L. Cai, and M. Yang, "An enhanced distributed acoustic sensor with large temperature tolerance based on ultra-weak fiber Bragg grating array," *IEEE Photon. J.*, vol. 12, no. 4, pp. 1–11, Aug. 2020.
[31] A. Fan, "Theoretical and experimental investigation on thermophysical problems in resources-environment-plant system," Ph.D. dissertation, School Energy Power Eng., Huazhong Univ. Sci. Technol., Wuhan, China, 2004.
[32] Y. Chen, Y. Wang, and Z. Mo, "Modeling for initial soil temperature," *J. Hunan Univ. Natural Sci.*, vol. 34, no. 7, pp. 27–29, 2007.

GUOLI LI was born in Binzhou, Shandong, in 1973. He received the B.Eng. degree in electrical engineering from the Zhengzhou University of Technology, Zhengzhou, China, in 1997, the M.Eng. degree in electrical engineering from Yanshan University, Qinhuangdao, China, in 2001, and the Ph.D. degree in agricultural electrification and automation from Nanjing Agricultural University, Nanjing, China, in 2017. He is currently an Associate Professor with the School of Mechanical and Electrical Engineering, Jinling Institute of Technology. He has authored or coauthored over 30 refereed technical articles, two books, and holds six patents in his areas of interests. His current research interests include optical fiber sensing technology, robotics, and intelligent control.

HENG ZHAO is currently pursuing the B.Eng. degree in electrical engineering and automation with the School of Mechanical and Electrical Engineering, Jinling Institute of Technology, with strong hands-on development ability. During the university, he actively participated in the research projects of his tutor, published two articles and obtained three software copyrights. His main research interests include optical fiber sensing technology and embedded control technology. He received many awards in the national robot related competitions.

FEI FENG is currently pursuing the B.Eng. degree in mechanical engineering and automation with the School of Mechanical and Electrical Engineering, Jinling Institute of Technology, with strong hands-on development ability. During the University, he actively participated in the research projects of his tutor, published four articles and obtained two software copyrights. His main research interests include optical fiber sensing technology and robotics. He received many awards in the national robot related competitions.

QIYUE WU is currently pursuing the B.Eng. degree in electrical engineering and automation with the School of Mechanical and Electrical Engineering, Jinling Institute of Technology, with strong hands-on development ability. During the University, he actively participated in the research projects of his tutor. His main research interests include robotics and embedded control technology. He received many awards in the national robot related competitions.

BO WEI received the B.Eng. degree in electronic information engineering from Hefei University, Hefei, China, in 2008, the M.Eng. degree in microelectronics and solid state electronics from the Yanshan University, Qinhangdao, China, in 2011. He is the General Manager of Wuxi Brillouin Electronic Technology Company Ltd., China. His current research interests include application of optical fiber sensing technology and application of intelligent control technology.